Quantification of detachment forces on rigid biofilm colonies in a roto-torque reactor using computational fluid dynamics tools

R. Sudarsan*, K. Milferstedt, E. Morgenroth**,*** and H.J. Eberl***

*Department of Mathematics and Statistics, University of Guelph, Guelph, Ontario, N1G 2W1, Canada (E-mail: *rsudarsa@uoguelph.ca; heberl@uoguelph.ca*)

**Department of Civil and Environmental Engineering, University of Illinois at Urbana-Champaign, Urbana, IL 61801, USA (E-mail: *milferst@uiuc.edu*)

***Department of Animal Sciences, University of Illinois at Urbana-Champaign, Urbana, Illinois 61801, USA (E-mail: *emorgenr@uiuc.edu*)

Abstract External detachment forces acting on evenly spaced biofilm colonies grown in a roto-torque reactor are calculated numerically using a finite element based 2-D CFD tool. The 2-D laminar shear flow around a biofilm colony is investigated for different shear rates corresponding to different rotating velocities of a roto-torque reactor. The effect of neighbouring biofilm colonies is accounted for by the choice of boundary conditions for the flow model. The forces acting on the biofilm colonies show an initial gradual increase as the spacing decreases from a large value up to a particular spacing beyond which they decrease rapidly with decreasing spacing. This trend is highly correlated with the detailed structure of the flow around the biofilm colonies.

Keywords Biofilm; computational fluid dynamics; detachment; hydrodynamics; shear forces

Water Science & Technology **Vol 52 No 7 pp 149–154** © IWA Publishing 2005

Introduction

Biofilm detachment is considered as an important factor for biofilm structure (van Loosdrecht *et al.*, 1995). It occurs as a response to increased external shear (Stoodley *et al.*, 2001; Choi and Morgenroth, 2003) or decreased internal strength, due to hydrolysis or starvation (Sawyer and Hermanowicz, 2000; Delaquis *et al.*, 1989; Wrangstadh *et al.*, 1989). Biomass is believed to detach when the tensile forces caused by the external shear exceed the tensile strength of the EPS matrix that holds together the biofilm (Ohashi and Harada, 1994; Kwok *et al.*, 1998) where the tensile strength of the biomass matrix depends on physical conditions inside the biofilm. The current paper attempts to estimate and understand the mechanical forces acting on the biofilm colonies under different physical flow conditions. The dominating factor controlling the external shear force is the advective flow velocity in the surrounding aqueous phase. However, the local flow velocity around the biofilm colonies is not only determined by the bulk flow, but it also depends on the morphology of the biofilm (De Beer and Stoodley, 1995). Therefore, in recent years much effort has been dedicated to the effects of detachment forces on the morphology of biofilms (Rittmann, 1982; Tijhuis *et al.*, 1996; Gjaltema *et al.*, 1997; Kwok *et al.*, 1998).

Biofilms grown at higher flow velocities have been shown to be denser than those grown at lower velocities. Many studies (e.g., Beyenal and Lewandowski, 2002; Peyton, 1996) have concluded that, depending on the flow velocity under which they are grown, biofilms arrange their internal structure to optimize the nutrient transport rate and their mechanical strength needed to resist detachment. These studies indicate that biofilms grown at low velocities exhibit low density and high effective diffusivity or mass transfer rate but cannot resist detachment due to high shear stress, while biofilms grown at higher velocities are denser and able to resist higher shear stress but with low effective

diffusivity. As suggested by Stoodley *et al.* (1999), the nature of the flow or fluid shear acting on individual cell clusters in a heterogeneous biofilm will be more complex than for a planar biofilm. It was proposed that the nature of the flow around biofilm colonies is a function of the extent of surface coverage of substratum by biofilm colonies. At low densities of spatial distribution of clusters (clusters far apart), the velocity profile between the clusters recovers downstream of each biofilm cluster, while at high densities (closely placed clusters) a 'wake interaction flow' occurs.

We compute the shear forces acting on the biofilm colonies at different levels of clustering and at different flow velocities and try to quantitatively determine the extent to which clustering of biofilm colonies influences the mechanical forces acting on the individual biofilm colonies in the cluster. We numerically solve for the 2-D flow around biofilm colonies (assumed to be rigid and non-growing) with prescribed morphology and uniform spatial distribution on the substratum. Despite the simplifying assumptions on the morphology this investigation sheds light on the structure of the flow between biocolonies as well as on the influence that clustering has on the shear forces acting on individual colonies. Picioreanu *et al.* (2000) included such a shear force computation in an ad hoc mechanistic model of biofilm detachment, which was incorporated in a 2-D growth model. We compute the shear forces in 2-D biofilms using a refined and more accurate body conforming grid and systematically investigate the influence of different spacing between biofilm colonies at different flow velocities. The primary objective of this paper is to estimate the effect that clustering of biofilm colonies has on the net forces acting on an individual colony.

Methods

Detailed examination of biofilms grown under different flow conditions using NMR (e.g. Lewandowski *et al.*, 1993) and CSLM (De Beer *et al.*, 1994a, b; Stoodley *et al.*, 1994) have revealed that biofilms are heterogeneous structures consisting of cell clusters separated by channels that enhance water flow through biofilms. Three-dimensional reconstruction of biofilm morphologies (Lewandowski *et al.*, 1995) from CSLM images indicates that to a first-order approximation, the shapes of the biofilm clusters can be approximated by a stretched ellipsoid chopped off at the base, or by a stretched sinusoidal profile. We use the latter to represent the shape of an individual biofilm colony. Such a biofilm colony (Figure 1) is characterized by its aspect ratio $A = W/H$, where W is the width of the colony at the substratum and H is its maximum height over the substratum. Biofilm clusters are assumed to consist of colonies of the same shape and size and have

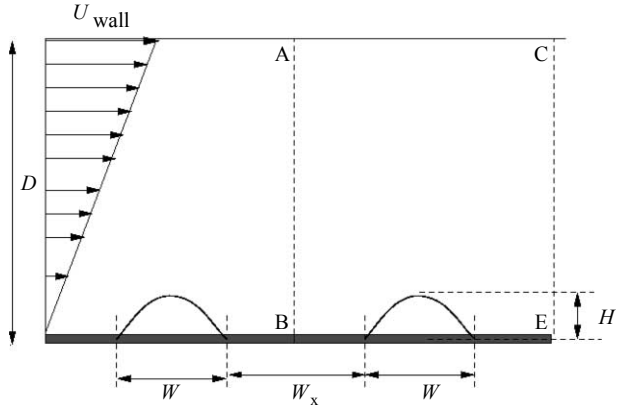

Figure 1 Schematic showing the flow configuration. A biofilm colony is represented by a sinusoidal object of width W and height H. The distance between neighbouring colonies is W_X. For the simulation it is sufficient to consider the rectangular domain ACEB. The shear rate G is determined by the ratio of U_{wall} and D

uniform spacing W_X (cf. Figure 1). The shear flow over the biofilm clusters in a roto-torque reactor is characterized by the shear rate, G, which is a measure of the normal velocity gradient at the substratum. Such a shear flow with a given shear rate is mimicked in our simulations by moving a plate at a distance D from the substratum with a velocity U_{wall} parallel to the substratum, such that $G = U_{\text{wall}}/D$. By choosing $D \gg W$, we can ensure that the flow established over the biofilm is a good approximation of the shear flow present over the biofilm colonies on the wall of the roto-torque reactor like the one used in Choi and Morgenroth (2003). This Couette mechanism for driving the flow has been used in biofilm simulation studies before (e.g. Eberl *et al.*, 2000) and was discussed there. The governing equations are the unsteady incompressible Navier–Stokes equations describing conservation of mass (1) and conservation of momentum (2),

$$\nabla \cdot \vec{u} = 0 \tag{1}$$

$$\frac{\partial \vec{u}}{\partial t} + \vec{u} \cdot \nabla \vec{u} = -\frac{1}{\rho} \nabla p + \nu \nabla^2 \vec{u} \tag{2}$$

where $\vec{u}$ is the velocity vector with components in x-direction (along the substratum) and z-direction (perpendicular to the substratum), p is the dynamic pressure field and constants ρ and ν are respectively the density and kinematic viscosity of the aqueous phase. The equations are solved using a penalty function based finite element method with semi-implicit time integration; details are given in Heinrich and Pepper (1999). For our study, their original code was modified to include periodic boundary conditions in x-direction, i.e. the inflow and outflow velocity are identical. This mimics a long, self-repeating biofilm cluster (cf. Eberl *et al.*, 2000). Thus, it is sufficient to simulate the flow past one biofilm colony (domain ABCE in Figure 1). A no-slip boundary condition ($\vec{u} = 0$) is used at the substratum and along the biofilm/water interface. The chosen finite element method uses 4-noded iso-parametric quadrilateral elements with bilinear interpolation of velocity and assumes a constant pressure inside each element. The computational grid is smoothly adapted to the biofilm structure, thus allowing for a much more accurate computation of the flow field close to the liquid/biofilm interface (and hence shear forces), than in previous CFD studies of biofilms (e.g. Bungartz *et al.*, 2000; Eberl *et al.*, 2000; Picioreanu *et al.*, 2000) that were based on a simple uniform voxel discretization. The numerical experiment is conducted for three different shear rates G, namely 100, 500 and 1,000 s^{-1}. These shear rates correspond to a Reynolds number (Re) of 25, 125 and 250 respectively, where $\text{Re} = U_{\text{wall}} W/\nu$. The influence of clustering is studied by flow simulations for different values of W_X/W at a given value of W/H. The shear force (tangential and normal) acting on the biofilm surface is calculated from the computed flow velocities and pressure distribution. The net force acting on the biofilm parallel to the substratum (F_X, also called the drag force) and normal to it (F_Z, also called the lift force) are then determined as

$$(F_X, F_z) = \oint_S \sigma \cdot \vec{n}\, ds \tag{3}$$

where σ is the shear stress tensor, $\vec{n}$ is the unit vector normal to the biofilm–liquid interface. The integral in (3) is taken over the surface of the colony.

Results and discussion

In all simulations the flow attained a steady state. At high shear rates G of 500 and 1,000 s^{-1} the flow around the biofilm colony separates on the downstream side of the biofilm colony and forms a re-circulating eddy. The location where this separation occurs varies and depends on the spacing between the biofilm colonies. This downstream

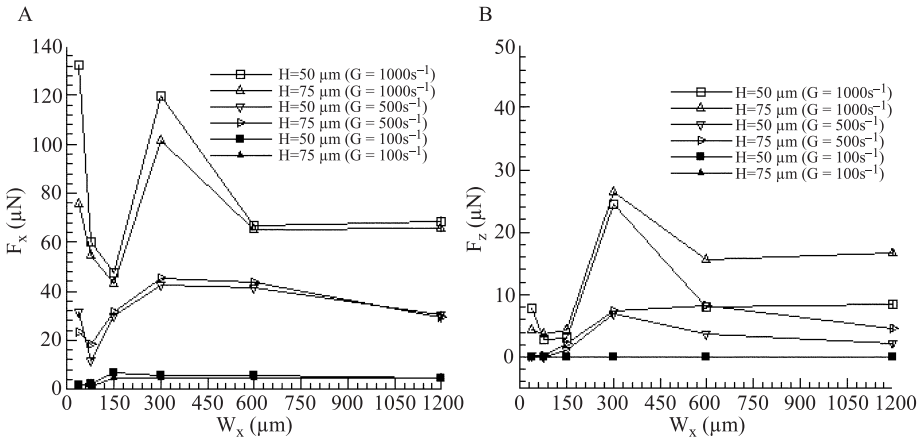

Figure 2 Drag force F_X and lift force F_Z acting on a sinusoidal colony with $H = 50{,}75$ μm, $W = 100$ μm for different spacings between the biofilm colonies at different shear rates

re-circulating zone corresponds to a region of low pressure. Its formation and growth in size results in increased pressure difference between the upstream side and downstream side of the biofilm colony, resulting in an increased drag force. Net drag force F_X and lift force F_Z are plotted in Figure 2 for different spacing at a shear rate of 100, 500 and $1{,}000\,s^{-1}$. The drag force F_X increases as expected with increasing G at all spacings between the biofilm colonies. The lift force F_Z is a small fraction of the drag force and its value increases as the height of the biofilm colony increases from 50 to 75 μm. The drag force on the colony decreases slightly as the height of the colony increases from 50 to 75 μm for all W_X. This is accompanied by an increase in the lift force. At very large W_X and large H/W our system is similar to flow around a single surface mounted blunt bluff body as studied by Bhattacharya *et al.* (2001) where the same trend was observed. Our simulation experiments extend this observation also to smaller W_X.

Effect of spacing: For $G = 500\,s^{-1}$ and $1{,}000\,s^{-1}$, the drag force increases (gradually for $G = 500\,s^{-1}$and steeply for $G = 1{,}000\,s^{-1}$) as the spacing between the biofilm colonies is decreased from 1,200 to 300 μm. This is a consequence of an increasing pressure difference between the upstream and downstream sides and is correlated with the growing size of the re-circulating zone (i.e., increased Z_{sep}) (Figure 3A and B). As the spacing decreases from 300 μm a re-circulating zone begins to develop also upstream of the biofilm colony (Figure 4A), accompanied by a decrease of the drag force and an increase of the lift force. As the spacing is reduced further, the downstream eddy of one biofilm colony begins to interact with the upstream eddy of the subsequent colony. Eventually both merge and form one eddy (Figure 4B). Once these two zones are merged with further decrease in spacing the drag force is seen to increase rapidly. This rapid increase at close spacings is a result of a strong re-circulating flow (back eddy) being established in the narrow void between the colonies. This is an artifact of the 2D simulation and should be bypassed by a 3D flow simulation as the strength of this circulation or the wake in 3D is expected to be significantly weaker than what is predicted in a 2D flow. This warrants the need for 3D simulations to correctly evaluate the shear forces acting on closely placed colonies.

Conclusions

The flow simulations carried out in this study show the complex hydrodynamic interactions of individual colonies in a biofilm system. Dependent on the distance between the colonies, their size and shape, and the bulk flow velocity, re-circulation zones

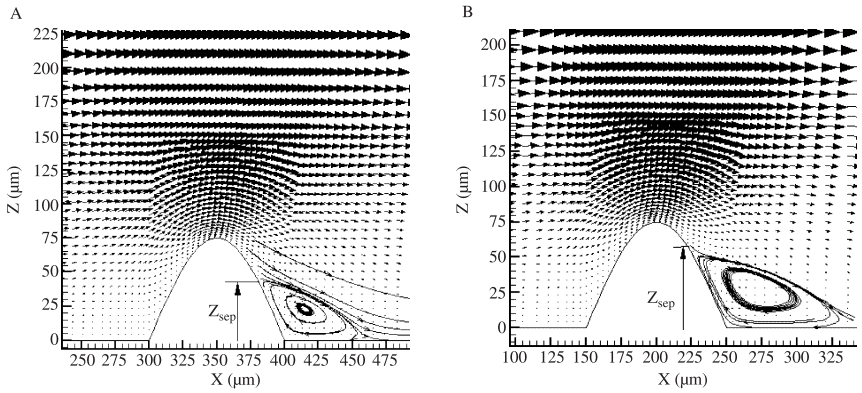

Figure 3 Vector plot of the flow over a biofilm colony ($H = 75$ μm) at a shear rate of 1,000 s^{-1} for spacing 600 μm (A) and 300 μm (B). Stream traces are shown to mark the downstream re-circulating zone along with flow separation location Z_{sep}. The extent of the domain in the x-direction shown in the figures does not correspond to the full extent of computational domain in x.

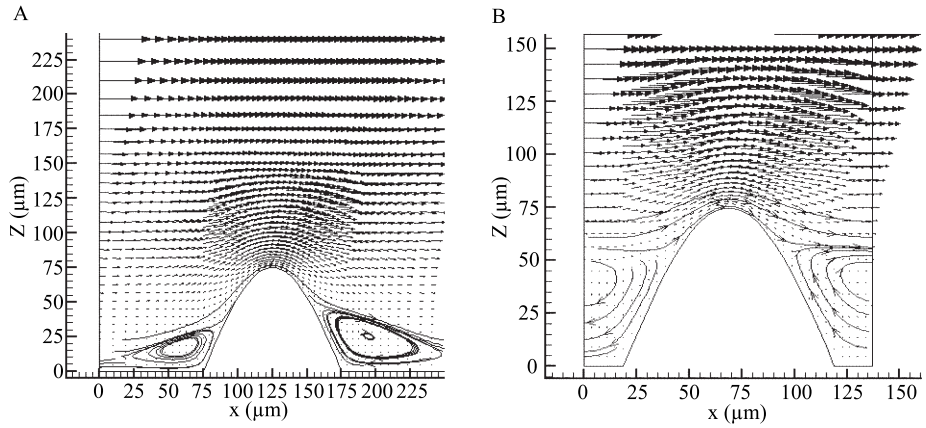

Figure 4 Vector plot of the flow over a biofilm colony ($H = 75$ μm) at a shear rate of 1,000 s^{-1} for spacing 150 μm (A) and 75 μm (B)

develop. In these, the hydrodynamic pressure is low and the flow reverses its direction. This has a notable effect on the external detachment forces acting on the individual biofilm colonies. The simulations imply that a biofilm colony is exposed to the highest detachment forces if the distance to the neighbouring colonies is on the order of 30–50 μm (due to a strong eddy driven by bulk flow). Another extreme value is observed at a distance approximately three times the size of the colony itself (due to increasing size of the downstream eddy). For larger distances between neighbouring colonies the detachment forces decline as the flow field recovers. The best protection against detachment is observed at a distance between the two extreme cases (due to formation of an upstream eddy). The 2-D simulations in this study correspond to flow over ripples of biofilms. In order to investigate detachment forces in patchy biofilms, more demanding 3-D computations must be carried out.

Acknowledgements

This study was supported by the Volkswagen Stiftung, Hannover, Germany with a grant in the funding program *Young Academics In Interdisciplinary Environmental Research* awarded to HJE and by a CAREER award to EM from the National Science Foundation under grant No. BES-0134104.

References

Beyenal, H. and Lewandowski, Z. (2002). Internal and external mass transfer in biofilms grown at various flow velocities. *Biotech. Prog.*, **18**(1), 55–61.

Bhattacharyya, S., Dennis, S.C.R. and Smith, F.T. (2001). Separating shear flow past a surface mounted blunt obstacle. *J. Eng. Mech.*, **39**, 47–62.

Bungartz, H.J., Kuehn, M., Mehl, M., Hausner, M. and Wuertz, S. (2000). Fluid flow and transport in defined biofilms: experiments and numerical simulations on a microscale. *Wat. Sci.Tech.*, **41**(4/5), 331–338.

Choi, Y.C. and Morgenroth, E. (2003). Monitoring biofilm detachment under dynamic changes in shear stress using laser-based particle size analysis and mass fractionation. *Wat. Sci. Tech.*, **47**(5), 69–76.

De Beer, D., Stoodley, P. and Lewandowski, Z. (1994a). Effects of biofilm structures on oxygen distribution and mass transport. *Biotech. Bioeng.*, **43**(11), 1131–1138.

De Beer, D., Stoodley, P. and Lewandowski, Z. (1994b). Liquid flow in heterogeneous biofilms. *Biotech. Bioeng.*, **44**(5), 636–641.

De Beer, D. and Stoodley, P. (1995). Relation between the structure of an aerobic biofilm and transport phenomena. *Wat. Sci. Tech.*, **32**(8), 11–18.

Delaquis, P.J., Caldwell, D.E., Lawrence, J.R. and McCurdy, A.R. (1989). Detachment of Pseudomonas fluorescence from biofilms on glass surfaces in response to nutrient stress. *Microb. Ecol.*, **18**, 199–210.

Eberl, H.J., Picioreanu, C., Heijnen, J.J. and van Loosdrecht, M.C.M. (2000). A three-dimensional numerical study on the correlation of spatial structure, hydrodynamic conditions, and mass transfer and conversion in biofilms. *Chem. Eng. Sci.*, **55**, 6209–6222.

Gjaltema, A., Vinke, J.L., van Loosdrecht, M.C.M. and Heijnen, J.J. (1997). Abrasion of suspended biofilm pellets in airlift reactors: Importance of shape, structure and particle concentrations. *Biotech. Bioeng.*, **53**, 88–89.

Heinrich, J.C. and Pepper, D.W. (1999). *Intermediate Finite Element Method: Fluid Flow and Heat Transfer Applications*, Taylor & Francis, New York.

Kwok, W.K., Picioreanu, C., Ong, S.L., van Loosdrecht, M.C.M., Ng, W.J. and Heijnen, J.J. (1998). Influence of biomass production and detachment forces on biofilm structures in airlift suspension reactor. *Biotech. Bioeng.*, **58**(4), 400–407.

Lewandowski, Z., Altobelli, S.A. and Fukushima, E. (1993). NMR and microelectrode studies of hydrodynamics and kinetics in biofilms. *Biotech. Prog.*, **9**(1), 40–45.

Lewandowski, Z., Stoodley, P. and Altobelli, S. (1995). Experimental and conceptual studies on mass transport in biofilms. *Wat. Sci. Tech.*, **31**(1), 153–162.

Ohashi, A. and Harada, H. (1994). Characterization of detachment mode of biofilm developed in an attached growth reactor. *Wat. Sci. Tech.*, **30**(11), 35–45.

Peyton, B.M. (1996). Effects of shear stress and substrate loading rate on *Pseudomonas aeruginosa* biofilm thickness and density. *Wat. Res.*, **30**(1), 29–36.

Picioreanu, C., van Loosdrecht, M.C.M. and Heijnen, J.J. (2000). Two-dimensional model of biofilm detachment caused by internal stress from liquid flow. *Biotech. Bioeng.*, **72**(2), 205–218.

Rittmann, B.E. (1982). The effect of shear stress on biofilm loss rate. *Biotech. Bioeng.*, **24**, 501–506.

Sawyer, L.K. and Hermanowicz, S.W. (2000). Detachment of *Aeromonas hydrophila* and *Pseudomonas aeruginosa* due to variations in nutrient supply. *Wat. Sci. Tech.*, **41**(4–5), 139–145.

Stoodley, P., de Beer, D. and Lewandowski, Z. (1994). Liquid flow in biofilm systems. *Appl. Environ. Microbiol.*, **60**, 2711–2716.

Stoodley, P., Dodds, I., Boyle, J.D. and Lappin-Scott, H.M. (1999). Influence of hydrodynamics and nutrients on biofilm structure. *J. Appl. Microbiol.*, **85**, 19S–28S.

Stoodley, P., Wilson, S., Stoodley, L.H., Boyle, J.D., Lapin-Scott, H.M. and Costerton, J.W. (2001). Growth and detachment of cell clusters from mature mixed species biofilms. *Appl. Env. Microbiol.*, **67**(12), 5608–5613.

Tijhuis, L., Hijman, B., van Loosdrecht, M.C.M. and Heijnen, J.J. (1996). Influence of detachment, substrate loading and reactor scale on the formation of biofilms in airlift reactors. *Appl. Microbiol. Biotech.*, **45**, 7–17.

van Loosdrecht, M.C.M., Eikelboom, D., Gjaltema, A., Mulder, A., Tijhuis, L. and Heijnen, J.J. (1995). Biofilm structures. *Wat. Sci. Tech.*, **32**(8), 35–43.

Wrangstadh, M., Conway, P.L. and Kjelleberg, S. (1989). The role of an extracellular polysaccharide produced by the marine Pseudomonas sp.S9 in cellular detachment during starvation. *Can. J. Microbiol.*, **35**(2), 309–312.